

Effects of inclined baffle location and Prandtl number on natural convection in a cavity

F. OZGEN^{*,1} Y. VAROL² H. F. OZTOP³

² Firat University, Department of Automotive Engineering, Technology Faculty, 23119 Elazig, Turkey

³ Firat University, Department of Mechanical Engineering, Technology Faculty, 23119 Elazig, Turkey

*filizozgen@gmail.com

(Received: 06.06.2014; Accepted: 01.10.2014)

Abstract

The problem of steady, laminar, conjugate-natural convection in a square cavity with an adiabatic baffle mounted on a vertical wall at different positions is formulated. In this study, natural convection heat transfer in a square cavity with an adiabatic fin mounted on a vertical wall was investigated numerically. Navier-Stokes equations have been performed and they are solved using finite difference method (FDM). Results are obtained for various parameters as the baffle location ($0.25 \leq h \leq 0.75$), thickness ($t=0.033$), length of baffle ($0.25 \leq w \leq 0.75$), Rayleigh numbers ($10^3 \leq Ra \leq 10^6$). Prandtl number values are $Pr=0.7, 1$ and 7 , is investigated. Results were presented with streamlines, isotherms, local and mean Nusselt numbers. It was found that Prandtl number and presence of the baffle on the wall have significant effect on natural convection.

Keywords: Natural convection, square enclosure, inclined baffle, fin

Eğimli Engel Yerleşimi ve Prandtl Sayısının Kapalı Hacimdeki Doğal Taşınım Üzerine Etkileri

Özet

Bu çalışmada, düşey duvarına farklı pozisyonlarda adiabatik engel yerleştirilmiş kare bir hacimdeki laminar doğal taşınım ısı transferi formüle edilmiştir. Düşey duvarında engel bulunan kapalı hacimdeki ısı transferi nümerik olarak da incelenmiştir. Navier-Stokes denklemleri kullanılmış ve denklemler sonlu farklar metodu (FDM) ile çözülmüştür. Sonuçlar, engelin farklı yerleşimi ($0.25 \leq h \leq 0.75$), farklı kalınlığı ($t=0.033$), farklı uzunluğu ($0.25 \leq w \leq 0.75$) ve Rayleigh sayıları için ($10^3 \leq Ra \leq 10^6$) sunulmuştur. Prandtl sayısı değeri $0.7, 1$ ve 7 alınmıştır. Sonuçlar, akım çizgileri, sıcaklık profilleri, yerel ve ortalama Nusselt sayıları şeklinde gösterilmiştir. Prandtl sayısı ve engelin duvar üzerindeki konumunun, doğal taşınımı önemli derecede etkilediği görülmüştür.

Anahtar Kelimeler: Doğal taşınım, kare hacim, eğimli engel, plaka

1. Introduction

Natural convection in sealed enclosures is found in many engineering applications such as room or office of buildings, solar energy collection systems, heat exchanger and cooling of electronical devices. There are some fundamental studies in literature on natural convection applications [1-5]. In these studies, enclosures do not have any baffle or object inside the enclosure.

Control of heat transfer and fluid flow in any type of enclosures are important to consume less energy and enhance the system efficiency. There are many studies on control of heat transfer via

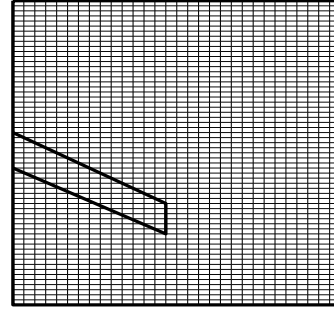
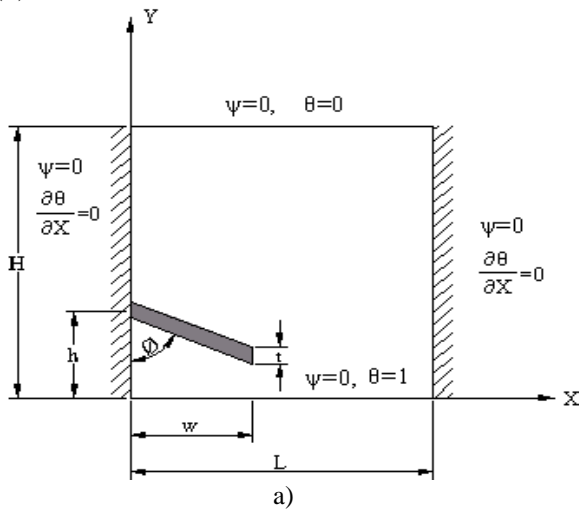
fin or baffle in literature. Shi and Khodadadi [6] analyzed the laminar natural convection in a differentially heated square cavity due to a thin fin on the hot wall. Effects of partial partition on both laminar and turbulent natural convection in enclosures are studied by Bilgen [7], numerically. In his case, vertical boundaries were isothermal at different temperature and horizontal boundaries were adiabatic. The results showed that the flow regime was laminar for Ra number up to 10^8 thereafter turbulent. Ben-Nakhi and Chamkha [8] studied the effect of length and inclination of a thin fin on natural convection in a square enclosure. A transverse temperature gradient is applied on two opposing walls of the

enclosure, while the other two walls are adiabatic. They reported that the Rayleigh number and the thin-fin inclination angle and length had significant effects on the average Nu number of the heated wall including the fin of the enclosure. Oztop et al. [9] investigated numerically effects of inclination angle on natural convection in an inclined open porous cavity with non-isothermally heated wall. It is found that inclination angle is the most important parameter on the temperature and flow field. Varol et al. [10] studied both experimentally and numerically natural convection heat transfer in an inclined fin attached square enclosure. It was observed that heat transfer can be controlled by attaching an inclined fin on to wall. Other related studies on baffle attached enclosure can be found in references as [11-20].

The study is focused on effects of location of inclined baffle and Prandtl number. Results will be presented by streamlines, isotherms, local and mean Nu numbers and velocity profiles at considered parameters.

2. Model

The schematic configuration of the considered geometry is shown in Fig. 1 (a) with boundary conditions and coordinates. It is a two dimensional square enclosure with an inserted inclined baffle. The length and thick of the baffle are shown by w and t , respectively. The enclosure is heated from bottom and cooled from top isothermally and vertical boundaries are adiabatic. Grid distribution is depicted in Fig. 1 (b).



b)

Figure 1. a) Schematic view of the square enclosure with baffle, coordinate system and boundary conditions, b) Grid distribution

1. Governing Equations

Two-dimensional Navier-Stokes equations with buoyancy forces are written in streamfunction-vorticity form in Eqs. (1) – (3). The mentioned equations are given for steady and laminar flow regime. The working fluid is accepted as incompressible and Newtonian. The Boussinesq approximation is applied. It is assumed that radiation heat exchange is negligible according to other modes of heat transfer and the gravity acts in vertical direction. Based on above assumptions, the governing equations are;

$$-\Omega = \frac{\partial^2 \Psi}{\partial X^2} + \frac{\partial^2 \Psi}{\partial Y^2} \quad (1)$$

$$\frac{\partial^2 \Omega}{\partial X^2} + \frac{\partial^2 \Omega}{\partial Y^2} = \frac{1}{\text{Pr}} \left(\frac{\partial \Psi}{\partial Y} \frac{\partial \Omega}{\partial X} - \frac{\partial \Psi}{\partial X} \frac{\partial \Omega}{\partial Y} \right) - \text{Ra} \frac{\partial \theta}{\partial X} \quad (2)$$

$$\frac{\partial \Psi}{\partial Y} \frac{\partial \theta}{\partial X} - \frac{\partial \Psi}{\partial X} \frac{\partial \theta}{\partial Y} = \frac{\partial^2 \theta}{\partial X^2} + \frac{\partial^2 \theta}{\partial Y^2} \quad (3)$$

The non-dimensional parameters are listed as

$$X = \frac{x}{L}, \quad Y = \frac{y}{L}, \quad \theta = \frac{T - T_c}{T_h - T_c}, \quad \Psi = \frac{\psi}{\alpha},$$

$$\Omega = \frac{\omega L^2 \text{Pr}}{\nu}, \quad U, V = \frac{(u - v)L}{\alpha},$$

$$u = \frac{\partial \Psi}{\partial y}, \quad v = -\frac{\partial \Psi}{\partial x}, \quad \text{Ra} = \frac{g \beta L^3 (T_h - T_c)}{\nu \alpha} \quad (4)$$

Boundary conditions for the considered model are depicted on the physical model as

shown in Fig. 1. In this model, the boundary conditions for all solid boundaries of enclosure and baffle are $U = V = 0$.

$$\text{On the bottom wall, } \theta(X,0)=1, \Psi(X,0)=0 \quad (5)$$

$$\text{On the top wall, } \theta(X,1)=0, \Psi(X,1)=0 \quad (6)$$

$$\text{On the vertical wall, } \frac{\partial\theta(0,Y)}{\partial X} = 0, \frac{\partial\theta(1,Y)}{\partial X} = 0, \\ \Psi(0,Y) = 0, \Psi(1,Y) = 0 \quad (7)$$

$$\text{On the baffle, } \frac{\partial\theta}{\partial n} = 0 \quad (8)$$

Local and mean Nusselt numbers are calculated along the bottom wall using Eqs. 9 (a) and 9 (b), respectively.

$$Nu_x = \left(-\frac{\partial\theta}{\partial Y} \right)_{Y=0} \quad (9a)$$

$$Nu = \int_0^1 Nu_x dX \quad (9b)$$

4. Numerical Method and Validation of Code

Central difference method (CDS) is applied to discretize the governing equations (1-3). The solution of linear algebraic equations was performed using Successive Under Relaxation (SUR) method. Thus, a code was developed using FORTRAN computer code. As convergence criteria, 10^{-4} is chosen for all dependent variables and value of 0.1 is taken for under-relaxation parameter. The number of grid points is taken as 61 x 61 with uniform spaced mesh in both X and Y directions. A table is presented to show the grid refinement test based on average Nu numbers. The listed data belongs to $\phi=45^\circ$, $Ra=10^4$, $h=0.5$, $t=0.033$, $w=0.3$, $RK=1$ and $Pr=0.71$. A regular grid distribution is used as shown in Fig. 1 (b). As it is well known from the theory of grid generation, the calculations for inclined boundaries are more difficult than that of vertical or horizontal boundaries. The reason is due to the fact that real boundaries are not coincided with mathematical domain. In this

study, the inclined walls were approximated with staircase-like zigzag lines. This technique is based on the earlier studies [19-22].

A grid test was performed as listed in Table 1 by changing grid dimensions from 21 x 21 to 91 x 91. It is observed that 61 x 61 grid is enough for this study. The numerical algorithm used in this study is tested with the classical differentially heated square enclosure problem. Natural convection heat transfer and fluid flow problem is investigated to get a comparison with literature. The obtained numerical results are compared with those given in different studies.

Table 1. Grid refinement test $\phi = 45^\circ$, $Ra = 10^4$, $h = 0.5$, $t = 0.033$, $w = 0.3$, $RK = 1$ and $Pr = 0.71$

| Grid Dimension | Nu |
|----------------|-------|
| 21x21 | 2.074 |
| 41x41 | 2.106 |
| 61x61 | 1.048 |
| 81x81 | 1.077 |
| 91x91 | 1.089 |

Table 2 presents a list on average Nu number from different earlier works and present study at different Ra numbers. Deviations are also presented in this table. The table clearly indicated that acceptable result is obtained. Another specific comparison has been performed against the result of Vahl Davis [1] based on streamlines and isotherms in Fig. 2 (a) and (b). The left one is obtained from present study and the right belongs to literature. They showed a very good agreement between those. Thus, it is decided that the problem is solvable with the written code.

Table 2. Comparison of results with literature including percentage of deviation

| Ra | 10^4 | 10^5 | 10^6 |
|----------------------------|----------------|----------------|----------------|
| Vahl Davis [1] | 2.243 (0.013%) | 4.519 (0.048%) | 8.800 (0.081%) |
| Vahl Davis and Jones [37] | 2.243 (0.013%) | 4.517 (0.049%) | 8.797 (0.08%) |
| Ben-Nakhi and Chamkha [12] | 2.244 (0.013%) | 4.524 (0.047%) | 8.856 (0.086%) |
| Present work | 2.272 | 4.738 | 8.086 |

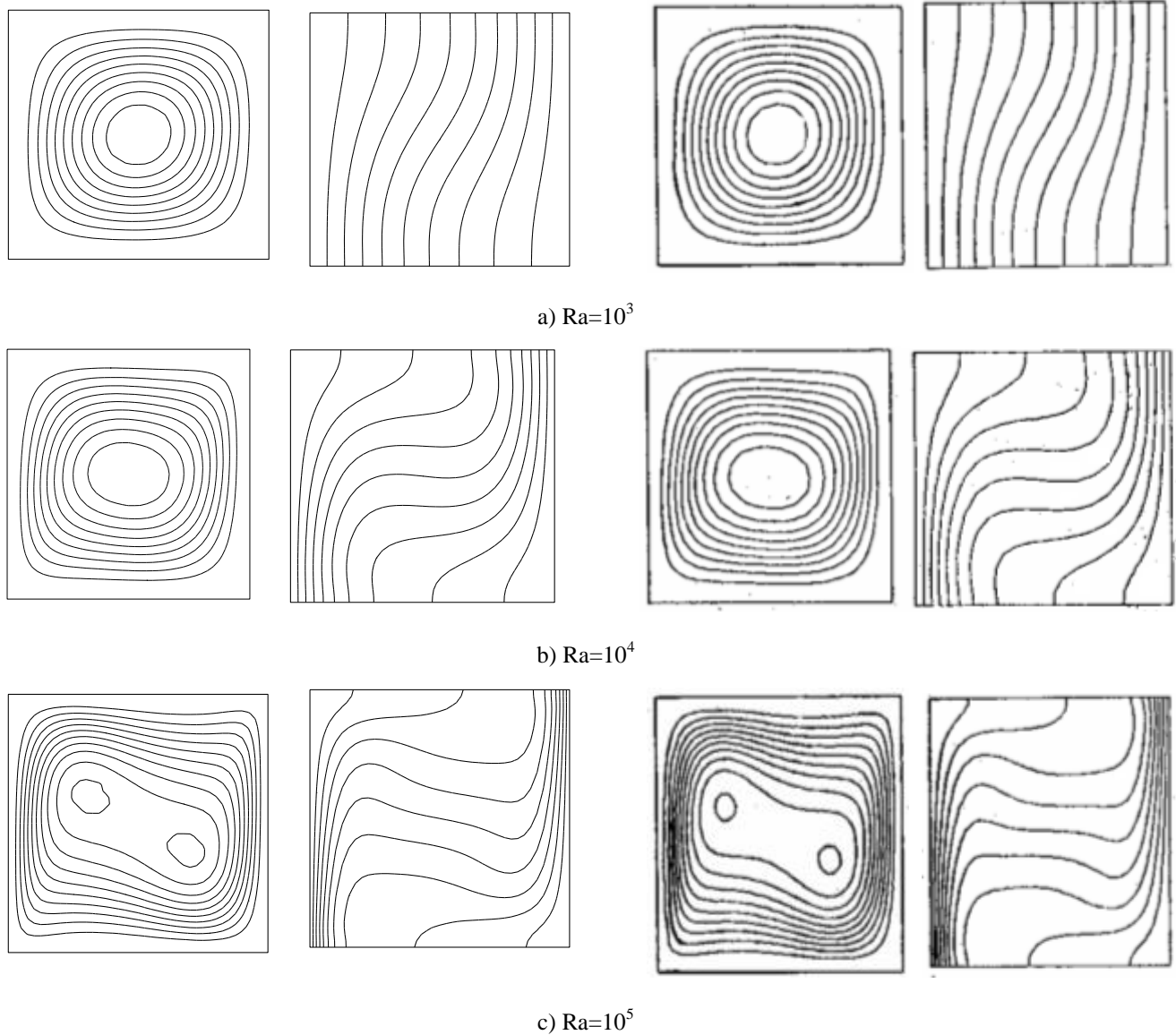


Figure 2. Comparison of stream and temperature functions with those of Vahl Davis (on the right) and present code (on the left), a) $Ra=10^3$, b) $Ra=10^4$, c) $Ra=10^5$

5. Results and Discussion

This study investigates the effects of Prandtl number and location of the inclined fin on heat and fluid flow in a square enclosure by using finite difference method. Obtained results will be presented by streamlines, isotherms, velocity profiles and Nu numbers for different parameters as given earlier sections.

Fig. 3 (a) and (b) show the streamlines (left column) and isotherms (right column) to see the effects of Prandtl number on temperature distribution and fluid flow at $\phi=60^\circ$, $Ra=10^5$, $h=0.5$, $t=0.033$, $w=0.5$ and $RK=1$. Generally,

there are two circulation cells were formed. The both cells rotate in same direction as counterclockwise. It is noted that the cavity is heated from the bottom and cooled from the ceiling. Thus, heated air moves toward to ceiling and the air impinge onto baffle. Flow strength decreases with decreasing of Prandtl number. The result indicates that variation of Prandtl number is not an important effective parameter on temperature distribution for low fluid velocity. Location of minimum stream function does not change with changing of Prandtl number due to narrow place under the baffle.

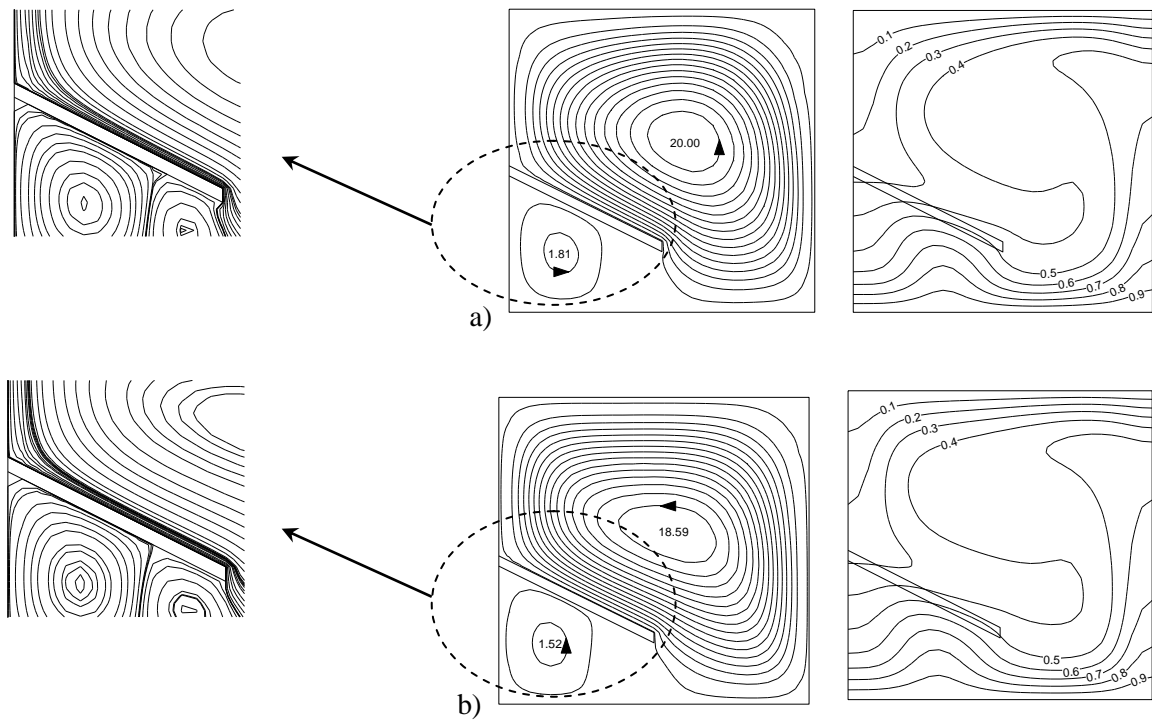


Figure 3. Streamlines (on the left) and isotherms (on the right) for $\phi = 60^\circ$, $Ra = 10^5$, $h = 0.5$, $t = 0.033$ and $w = 0.5$, a) $Pr = 1$, $\Psi_{\max}(0.5718,0.5728)=21.4$, $\Psi_{\min}(0.4009,0.1288)=-0.992$
 b) $Pr = 7$ ($\Psi_{\min}(0.4095,0.133)=-1.11$, $\Psi_{\max}(0.5589,0.56)=19.9$)

Effects of location of the baffle is presented in Fig. 4 (a) and Fig. 4 (b) for $h=0.25$ and $h=0.75$, respectively. In these figures, other

parameters are $\phi=60^\circ$, $Ra=10^5$, $t=0.033$, $w=0.25$, $RK=1$ and $Pr=0.71$. As it is seen from the streamlines, the short baffle with $h=0.25$ makes

small effect on flow field and single cell was formed in this case. When the location of baffle locates near the ceiling ($h=0.75$), two cells was observed inside the cavity. A kidney shaped main cell was formed and it rotates clockwise direction with $\Psi_{\min}(0.5461,0.5898) = -24$. The other small cell sits at the right bottom corner with $\Psi_{\max}=1.81$. It is an interesting observation that the location of the baffle makes a strong effect on flow direction and the baffle can control the flow direction. Besides, temperature of the middle part of the enclosure becomes almost constant for $h = 0.25$. Fig. 5 (a) and (b) illustrate the effect of baffle length on heat and

fluid flow for parameters $\phi=60^\circ$, $Ra=10^5$, $h=0.5$, $t=0.033$, $RK=1$ and $Pr=0.71$. Fig. 5 (a) plots the results for $w=0.25$ and it can be compared with Fig. 4. As it is seen that the second small cell locates under the baffle and the main cell hits it to the corner. Again, the rotation direction of the main cell is counterclockwise. The longer baffle divides the cavity into two parts as trapezoidal and triangle. Two cells are formed and they turn in same direction. Conduction mode of heat transfer becomes effective under the baffle due to slow flow motion. On the contrary, convection mode of heat transfer becomes dominant for short baffle.

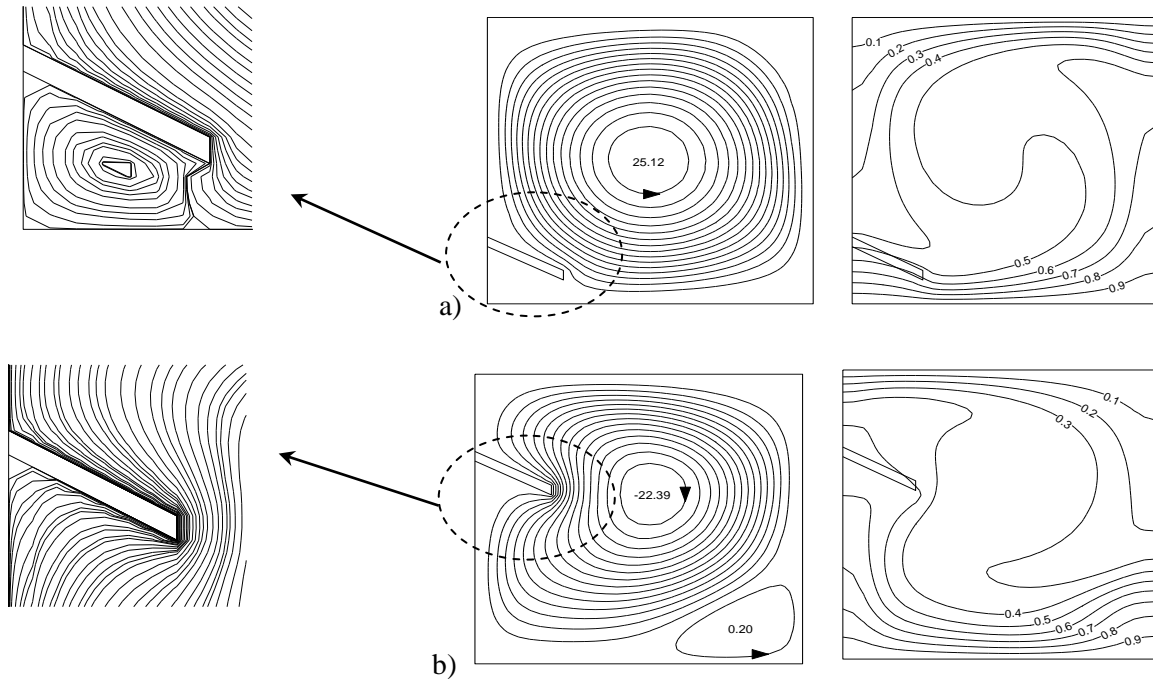


Figure 4. Streamlines (on the left) and isotherms (on the right) for $\phi = 60^\circ$, $Ra = 10^5$, $t = 0.033$, $w = 0.25$ and $Pr = 0.71$ a) $h_1 = 0.25$, $(\Psi_{\max}(0.4863,0.5002)=26.8, \Psi_{\min}(0.9346,0.9144)=-0.149)$
b) $h_2 = 0.75$ $(\Psi_{\max}(0.7981,0.1288)=1.81, \Psi_{\min}(0.5461,0.5898)=-24)$

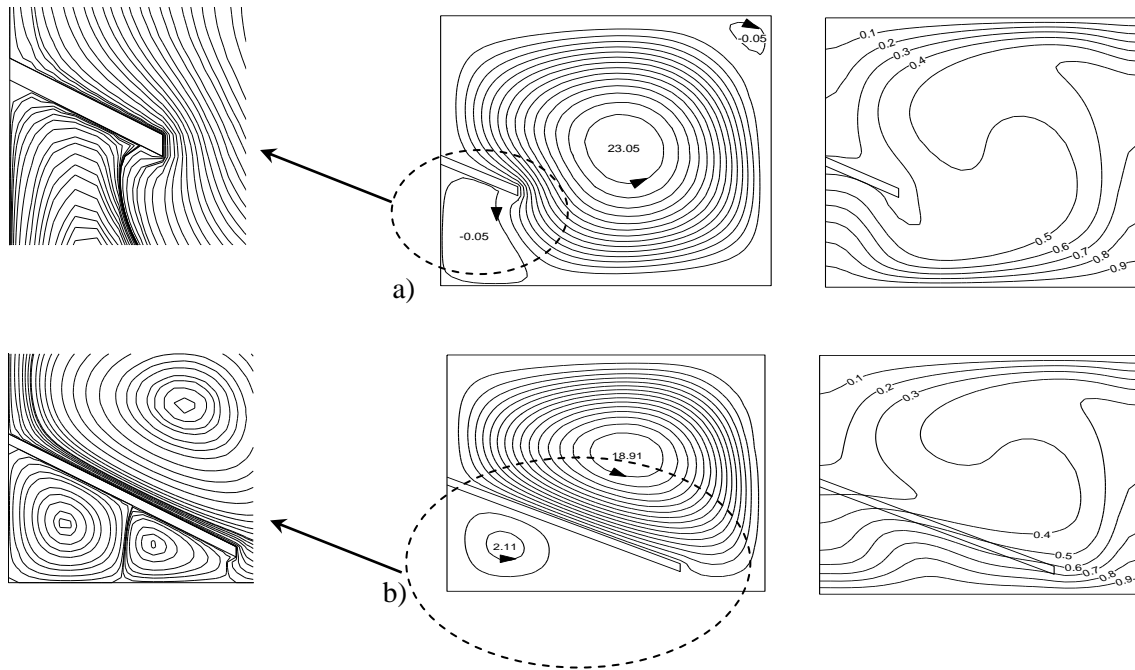


Figure 5. Streamlines (on the left) and isotherms (on the right) for $\phi = 60^\circ$, $Ra = 10^5$, $h = 0.5$, $t = 0.033$ and $Pr = 0.71$, a) $w_1 = 0.25$, $\Psi_{\max}(0.5546,0.5087)=24.7$, $\Psi_{\min}(0.1319,0.1501)=-1.7$
 b) $w_2 = 0.75$, $\Psi_{\max}(0.5632,0.5814)=20.2$, $\Psi_{\min}(0.4693,0.1245)=-0.475$

Fig. 6 presents the mean Nu number for different values of Pr number as a function of Ra number. The average Nu number becomes constant for low Ra number due to domination of conduction mode of heat transfer. Then, it increases with Ra number.

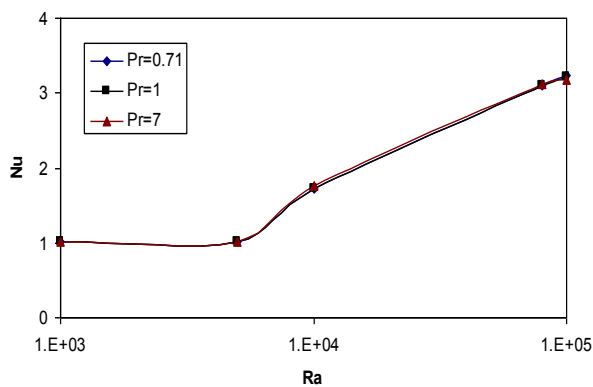
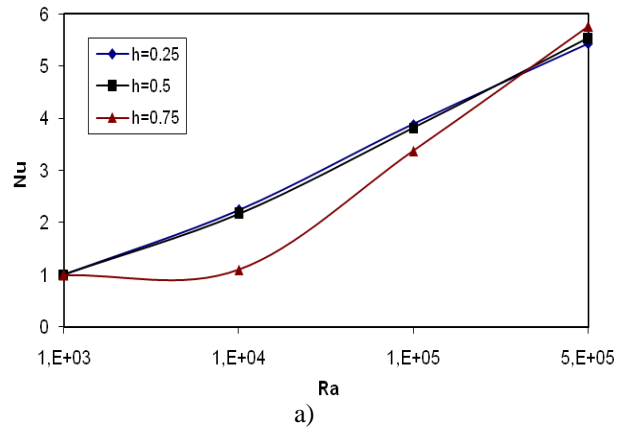


Figure 6. Variation of average Nusselt number with Ra number for $h=0.5$, $w=0.5$ and $t=0.033$

Fig. 7 (a) to (b) presents the average Nu number with Ra number for different values of Pr numbers at $w=0.25$ and $t=0.033$ to see the effects of location of baffle. The graphs show that the Pr number becomes an effective parameter based on location of the baffle. For $h=0.25$, heat transfer becomes lower than that of $h = 0.5$ and 0.75 for the highest value of Ra number. For other cases, there is a linear increasing on Nu number and Pr number effect becomes insignificant.



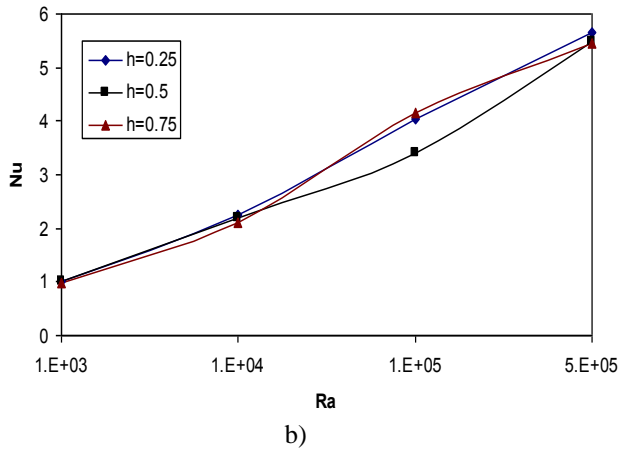


Figure 7. Variation of average Nu number with Ra number for $w=0.25$, $t=0.033$, a) $Pr=0.71$, b) $Pr=7$

Fig. 8 is illustrated the effects of baffle length on heat transfer for $h=0.5$, $t=0.033$ and $Pr=0.71$. In this case, there is a linear increasing with increasing of Ra number for all values of baffle length. The graphs indicate that the highest heat transfer is formed for the lowest value of baffle length. It means that the baffle can be a control parameter for heat transfer.

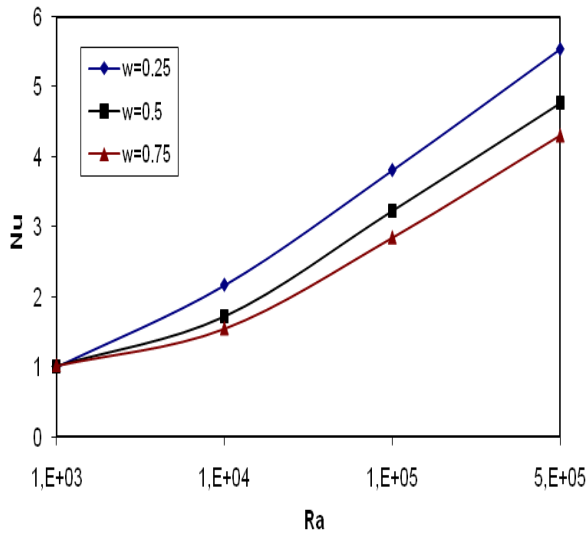


Figure 8. Variation of average Nusselt number with Ra number for $h=0.5$, $Pr=0.71$ and $t=0.033$

Fig. 9 (a) to (b) illustrates the effect of Pr number on trend of local Nu number variation on both hot and cold walls. Heat transfer increases from bottom to top and it has a maximum near the right vertical wall at the bottom wall. However, it shows a wavy variation along the

cold wall and it has a minimal point around $X=0.3$ and maximum for $X=0.6$. There is no big difference for different Pr numbers on both trend and values.

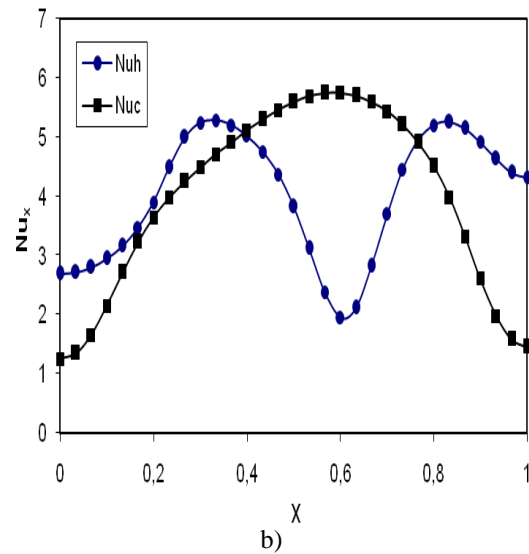
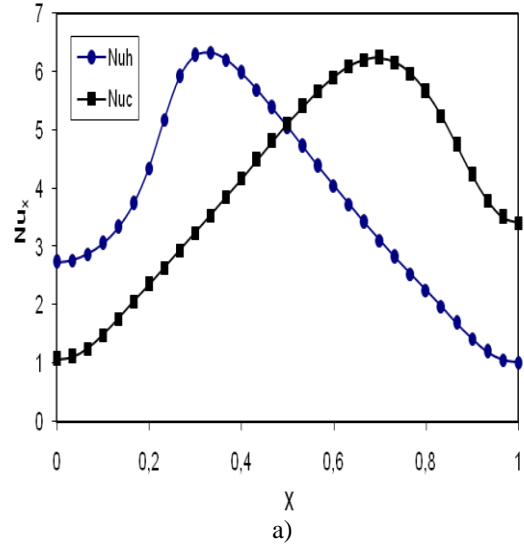


Figure 9. Variation of local Nusselt number with Rayleigh number for $h=0.25$, $w=0.25$, $t=0.033$ and $Ra=10^5$, a) $Pr=0.71$, b) $Pr=7$

Finally, Fig. 10 displays the variation of horizontal (Fig. 10 (a)) and vertical (Fig. 10 (b)) velocity profiles at different stations of the enclosure for $h=0.25$, $w=0.25$, $t=0.033$, $Pr=0.71$ and $Ra=10^5$. The negative velocity becomes high at $X=0.50$ and low at $X=0.25$. The velocities are not affected from the presence of the baffle at $X=0.75$ due to low velocity of the natural convection. Under the baffle, a small enclosure is formed (Fig. 10 (a)) and the flow circulates.

These results can be seen from streamlines as given above. Similarly, the presence of the baffle is only effective on flow at $Y=0.25$ and higher velocity is formed at the middle of the Y -axis and $X=0.90$.

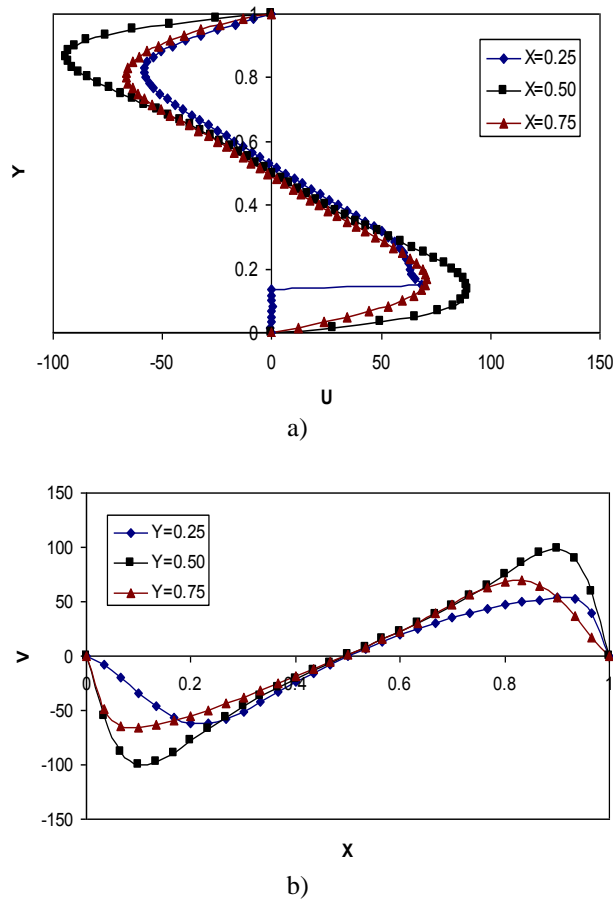


Figure 10. a) Horizontal velocity profile, b) Vertical velocity profile for $h = 0.25$, $w = 0.25$, $t = 0.033$, $Pr = 0.71$, $t = 0.033$, $\phi = 60$, $Ra = 10^5$.

6. Conclusion

A numerical study is performed to examine the natural convection heat transfer and fluid flow in square enclosure with adiabatic baffle attached. The governing equations in streamfunction-vorticity form are solved with finite difference technique and algebraic equations are solved using successive under relaxation (SUR) method. Thus, finite difference method is applied to inclined baffle. Graphical results for the streamline and temperature contours for various parametric conditions were

presented and discussed. It is found that the flow strength is decreased with increasing of Pr number. Location of the baffle is the most important parameters on flow field and temperature distribution. The location of baffle affects the main flow direction and number of cells. Heat transfer is decreased when the baffle locates near the ceiling. It can be a control parameter for temperature distribution and flow field. Pr number is not an important parameter for heat transfer especially at low flow velocities.

7. References

1. De Vahl Davis, G. (1983). Natural convection of air in a square cavity: A bench mark numerical solution. *International Journal Numer. Methot Fluids*, 3(3), 249-264.
2. Ostrach, S. (1972). Natural convection in enclosures. In *Advances in Heat Transfer* (Edited by J.P. Hartnett and T.F. Irvine). Academic Pres, 8, New York.
3. Bejan, A. (1982). *Convection Heat Transfer*. New York, Wiley.
4. Yang, K.T. (1987). Natural convection in enclosures. *Handbook of Single-Phase Heat Transfer*, Wiley, New York.
5. Catton, I. (1962). Natural convection in enclosures. *Proc. Sixth International Heat Transfer Conference*, 6, 13-31.
6. Shi, X. and Khodadadi, J.M. (2003). Laminar natural convection heat transfer in a differentially heated square cavity due to a thin fin on the hot wall. *Journal Heat Transfer*, 125(4), 624-634.
7. Bilgen, E. (2002). Natural convection in enclosures with partial partitions. *Renewable Energy*, 26(2), 257-270.
8. Ben-Nakhi, A. and Chamkha, A.J. (2006). Effect of length and inclination of a thin fin on natural convection in a square enclosure. *Numerical Heat Transfer*, 50(4), 381-399.
9. Oztop, H.F., Al-Salem, K., Varol, Y., Pop, I. and Firat, M. (2012). Effects of inclination angle on natural convection in an inclined open porous cavity with non-isothermally heated wall. *International Journal of Numerical Methods for Heat and Fluid Flow*, 22(8), 1053-1072.
10. Varol, Y., Oztop, H.F., Özgen, F. and Koca, A. (2012). Experimental and numerical study on laminar natural convection in a cavity heated from bottom due to an inclined fin. *Heat Mass Transfer*, 48(1), 61-70.
11. Tasnim, S.H. and Collins, M.R. (2004). Numerical analysis of heat transfer in a square

- cavity with a baffle on the hot wall. *International Comm. Heat Mass Transfer*, 31(5), 639-650.
12. Bilgen, E. (2005). Natural convection in cavities with a thin fin on the hot wall. *International Journal Heat Mass Transfer*, 48(17), 3493-3505.
 13. Dagtekin, I. and Oztop, H.F. (2001). Natural convection heat transfer by heated partitions within enclosure. *International Communication Heat Mass Transfer*, 28(6), 823-834.
 14. Famouri, M. and Hooman, K. (2008). Entropy generation for natural convection by heated partitions in a cavity. *International Comm. Heat Mass Transfer*, 35(4), 492-502.
 15. Frederick, R.L. (1989). Natural convection in an inclined square enclosure with a partition attached to its cold wall. *International Journal Heat Mass Transfer*, 32(1), 87-94.
 16. Acharya, S. and Jetli, R. (1990). Heat transfer due to buoyancy in a partially divided square box. *International Journal Heat Mass Transfer*, 33(5), 931-942.
 17. Turkoglu, H. and Yücel, N. (1996). Natural convection heat transfer in enclosures with conducting multiple partitions and side walls. *Heat and Mass Transfer*, 32(1-2), 1-8.
 18. Aydın, O. and Pop, I. (2007). Natural convection in a differentially heated enclosure filled with a micropolar fluid. *International Journal Thermal Science*, 46(10), 963-969.
 19. Varol, Y., Oztop, H.F. and Pop, I. (2010). Maximum density effects on buoyancy-driven convection in a porous trapezoidal cavity. *International Journal Heat Mass Transfer*, 37(4), 401-409.
 20. Haese, P.M. and Teubner, M.D. (2002). Heat exchange in an attic space. *International Journal Heat Mass Transfer*, 45(25), 4925-4936.
 21. De Vahl Davis, G.D. and Jones, I.P. (1983). Natural convection in a square cavity: A comparison exercise. *International Journal Num. Methot Fluids*, 3(3), 227-248.
 22. Oztop, H.F. and Bilgen, E. (2006). Natural convection in differentially heated and partially divided square cavities with internal heat generation. *International Journal Heat Fluid Flow*, 27(3), 466-475.